

WIND-POWERED ULTRALUMINOUS X-RAY SOURCES

GRZEGORZ WIKTOROWICZ^{1,2,3}, JEAN-PIERRE LASOTA^{3,4}, KRZYSZTOF BELCZYNSKI³, YOUJUN LU^{1,2}, JIFENG LIU^{1,2,5},
KRYSTIAN ILKIEWICZ^{3,6}

¹ National Astronomical Observatories, Chinese Academy of Sciences, Beijing 100101, China

² School of Astronomy & Space Science, University of the Chinese Academy of Sciences, Beijing 100012, China

³ Nicolaus Copernicus Astronomical Center, Polish Academy of Sciences, Bartycka 18, 00-716 Warsaw, Poland

⁴ Institut d'Astrophysique de Paris, CNRS et Sorbonne Université, UMR 7095, 98bis Bd Arago, 75014 Paris, France

⁵ WHU-NAOC Joint Center for Astronomy, Wuhan University, Wuhan, China

⁶ Department of Physics and Astronomy, Box 41051, Science Building, Texas Tech University, Lubbock, TX 79409-1051, USA

Draft version March 4, 2021

ABSTRACT

Although ultra-luminous X-ray sources (ULX) are important for astrophysics due to their extreme apparent super-Eddington luminosities, their nature is still poorly known. Theoretical and observational studies suggest that ULXs could be a diversified group of objects composed of low-mass X-ray binaries, high-mass X-ray binaries and marginally also systems containing intermediate-mass black holes, which is supported by their presence in a variety of environments. Observational data on the ULX donors could significantly boost our understanding of these systems, but only a few were detected. There are several candidates, mostly red supergiants (RSGs), but surveys are typically biased toward luminous near-infrared objects. Nevertheless, it is worth exploring if RSGs can be members of ULX binaries. In such systems matter accreted onto the compact body would have to be provided by the stellar wind of the companion, since a Roche-lobe overflow could be unstable for relevant mass-ratios. Here we present a comprehensive study of the evolution and population of wind-fed ULXs and provide a theoretical support for the link between RSGs and ULXs. Our estimated upper limit on contribution of wind-fed ULX to the overall ULX population is $\sim 75\text{--}96\%$ for young (< 100 Myr) star forming environments, $\sim 49\text{--}87\%$ for prolonged constant star formation (e.g., disk of Milky Way), and $\lesssim 1\%$ for environments in which star formation ceased long time (> 2 Gyr) ago. We show also that some wind-fed ULXs (up to 6%) may evolve into merging double compact objects (DCOs), but typical systems are not viable progenitors of such binaries because of their large separations. We demonstrate that, the exclusion of wind-fed ULXs from population studies of ULXs, might have lead to systematical errors in their conclusions.

Subject headings: stars: black holes, gravitational waves, binaries: general, X-ray: binaries, methods: numerical, methods: statistical, astronomical databases: miscellaneous

1. INTRODUCTION

Ultra-luminous X-ray sources (ULXs) are defined as point-like off-nuclear X-ray sources with luminosities exceeding $10^{39} \text{ erg s}^{-1}$ (for a recent review see Kaaret et al. 2017) and are, therefore, the brightest X-ray sources that are neither supernovae (SNe) nor active galactic nuclei. After their identification at the end of the previous century it was thought for a long time that ULXs contain intermediate-mass ($M \sim 10^2\text{--}10^4 M_\odot$) black holes (IMBHs Colbert & Mushotzky 1999) accreting at rates close to, or below their Eddington values. The dissenting view of King et al. (2001), who pointed out that there are no viable evolutionary scenarios leading to the formation of such systems and suggested instead that most ULXs are stellar-mass binaries accreting at super-Eddington rates, was largely ignored until Bachetti et al. (2014) discovered that the source M82 ULX-2 contains an X-ray pulsar. This observation and the subsequent observations of five other pulsating ULXs (PULXs) by Israel et al. (2017); Fürst et al. (2017); Carpano et al. (2018); Sathyaprakash et al. (2019); Rodríguez Castillo et al. (2020) lead to a change of paradigm and now it is universally believed that most (if not all) ULXs contain stellar-mass accretors. PULXs have been also ob-

served during giant outbursts of Be-X-ray binary stars (one in the Galaxy, see King & Lasota 2020, and references therein), but their luminosities are always less than $3 \times 10^{39} \text{ erg s}^{-1}$.

The choice of the threshold ULX luminosity at $10^{39} \text{ erg s}^{-1}$ is rather unfortunate, because it fails to separate the “standard” X-ray binaries (XRBs) from the “generic” ULX. Indeed, at least five transient galactic XRBs reach luminosities superior to $10^{39} \text{ erg s}^{-1}$ (Tetarenko et al. 2016). Middleton et al. (2015) suggest that one should take $3 \times 10^{39} \text{ erg s}^{-1}$ as the minimum luminosity defining ULXs whose nature is “contentious”, i.e., that could contain either stellar-mass accretors or IMBHs. The idea was to make sure that if the accretor is a black hole (BH), such a floor value would make sure that the apparent luminosity is super-Eddington but this suggestion does not take into account that it is now known that stellar evolution can produce BHs with masses $\gtrsim 30 M_\odot$ (Belczynski et al. 2010b; Abbott et al. 2016), and up to $50 M_\odot$ under favorable conditions (e.g. Belczynski 2020). Therefore, only sources with luminosities larger than $\sim 6 \times 10^{39} \text{ erg s}^{-1}$, say, can be expected to be (apparently) super-Eddington if they contain a stellar-





mass BH¹.

Since the isotropic luminosity of an accreting body can be, at best, few times its Eddington value (see, e.g. Shakura & Sunyaev 1973; Poutanen et al. 2007), observed luminosities $L \gg L_{\text{Edd}}$, where L_{Edd} is the Eddington luminosity, are only apparently super-Eddington and must be due to radiation beamed toward the observer (King et al. 2001; Abramowicz 2005). For example, in the model by King (2009) radiation is collimated for $L \gtrsim 3L_{\text{Edd}}$. One should realise that for neutron star (NS) accretors beaming of apparently super-Eddington luminosities is unavoidable. In the case of NS ULXs, it has been speculated that magnetar-strength magnetic field ($B > 10^{13}$ G), by increasing the value of the threshold luminosity, would make the emission effectively subcritical (cf Tong 2015; Dall’Osso et al. 2015; Ekşi et al. 2015; Mushtukov et al. 2015). However, this hypothesis is contradicted by observations in several ULXs of cyclotron resonance scattering feature (CRSF), which corresponds to magnetic fields $B \sim 10^{11} - 10^{12}$ G (Brightman et al. 2018; Middleton et al. 2019; Walton et al. 2018), as well as by the absence of magnetars in binary systems, which is consistently explained by their formation scenarios invoking the destruction of the parent binary system (see King & Lasota 2019, and references therein). The importance of beaming in the context of the ULX origin and observed populations was recently analysed by Wiktorowicz et al. (2019a).

Since the universal presence of extremely strong magnetic fields in NS ULXs is very unlikely and in BH ULXs impossible, the observed luminosities $\gtrsim 3 \times 10^{39} \text{ erg s}^{-1}$ for NU LXs (we allow for the existence of NSs with masses $\approx 2.5 M_{\odot}$, Abbott et al. 2020), and larger than $\sim 6 \times 10^{39} \text{ erg s}^{-1}$ in general, cannot be intrinsic and must be beamed, as predicted by King et al. (2001). This in turn requires high accretion rates² typically $\dot{m} \equiv \dot{M}/\dot{M}_{\text{Edd}} \gtrsim 9$, where $\dot{M}_{\text{Edd}} = 2.0 \times 10^{-8} M_{\star} (0.1/\eta) M_{\odot}/\text{yr}$, with η being the accretion efficiency and M_{\star} the accretor mass in solar units. Therefore, the accretion rate in bright ULXs ($L_{\text{X}} > 6 \times 10^{39} \text{ erg s}^{-1}$) should be larger than $\sim 1.8 \times 10^{-7} M_{\star} (0.1/\eta) M_{\odot}/\text{yr}$. This is roughly the minimum rate at which accretion discs in (quasi)steady ULXs must be fed by the companion star. Some ULXs are transient (see, e.g. Earnshaw et al. 2020; Brightman et al. 2020) and if this luminosity variability is due to the disc thermal-viscous instability the MT rate should be lower than the value mentioned above (Hameury & Lasota 2020).

The detection of a donor and its orbital motion can shed more light on the MT rates in a ULX and the nature of these objects. However, all ULXs, except potential Galactic ones like SS433 and the Be-X source Swift J0243.66124, are extra-galactic objects and their donors, if not very luminous, remain undetectable for contemporary surveys. Only in the case of two systems, companion stars were dynamically confirmed: 10–20 M_{\odot} B9Ia star in NGC7793 P13 (Motch et al. 2014) and $> 3.4 M_{\odot}$ WR star in NGC 101 ULX-1 (Liu et al. 2013). **Binary pop-**

ulation studies suggest that the majority of ULXs are powered by low-mass and low-luminous donors, which is consistent with the lack of detection of any companions in the majority of ULXs. For example, Wiktorowicz et al. (2017) showed that the majority of ULXs will harbour $M < 3 M_{\odot}$ MS donors. Such stars are observable only in the vicinity of the Sun (even HST is constrained to the Milky Way Galaxy in their case). Hyper-luminous X-ray sources, typically defined as ULXs with apparent luminosities above $10^{41} \text{ erg s}^{-1}$, are still viable candidates to harbour massive donors ($\gtrsim 10 M_{\odot}$; e.g. Wiktorowicz et al. 2015).

Several ULXs possess donor candidates spatially are coincident with X-ray sources. Most of them were detected through observations in near-infrared (NIR) spectral band. In this band, red supergiants (RSG) should easily overcome NIR emission from an accretion disk (Copperwheat et al. 2005). Therefore, these stars were of particular interest in most of the surveys (e.g. Heida et al. 2014; López et al. 2017, 2020). Although blue supergiants were, at first, perceived as viable candidates for donors in ULXs owing to their prevalence in star forming regions, where most of the ULXs are being found, it was later realised that the optical companions might be outshone by the emission from an irradiated accretion disk (e.g. Sutton et al. 2014) unless the separation is very large (Copperwheat et al. 2007). This bias toward high-luminosity NIR companions might be the reason behind the majority of the detected companion candidates being RSGs (e.g. Heida et al. 2019). It is further complicated by the fact that we cannot measure distances to ULXs and RSGs directly and the distance to the coinciding galaxy is used as a proxy.

Even if RSG donors form only a small fraction of the intrinsic ULX population, most of such binary companions cannot be Roche-lobe (RL) filling stars. For example, Wiktorowicz et al. (2017) estimated that only $< 1\%$ of all ULXs can be accompanied by supergiants if RLOF accretion is concerned exclusively. In binaries containing a compact object and a RSG companion the mass ratio is typically high ($q = M_{\text{don}}/M_{\text{acc}} > 3$), especially for a NS accretor, which makes the RLOF dynamically unstable (e.g. van den Heuvel et al. 2017) and leads to a common envelope phase (e.g. Ivanova et al. 2013).

One should stress, however, that $q > 3$ may not imply dynamical instability if the stellar envelope is radiative. In this case, which corresponds to the initial phase of Case B binary mass exchange, the MT rate occurs at the thermal (Kelvin-Helmholz) time scale (Kippenhahn & Weigert 1967; Kippenhahn et al. 1967) and is equal to

$$\dot{M} \equiv \frac{M_{\text{don},\star}}{t_{\text{KH}}} = 3.2 \times 10^{-8} \frac{R_{\text{don},\star} L_{\text{don},\star}}{M_{\text{don},\star}} M_{\odot} \text{ yr}^{-1}, \quad (1)$$

where $M_{\text{don},\star}$, $R_{\text{don},\star}$, and $L_{\text{don},\star}$ are the mass, radius and luminosity of the donor, and index \star designates solar units (Paczynski 1971). Such transfer mechanism might power the brightest ULXs (Wiktorowicz et al. 2017). We note, that some simulations predict a wider range of binary parameters that give stable mass transfer (Pavlovskii et al. 2017).

Previous theoretical studies mostly neglected a possibility that ULXs can be “fed” by stellar winds, because in general, stellar winds are fast and tenuous, so only

¹ The limit may be even higher for He-rich accretion and most massive BHs (e.g. Belczynski 2020)

² The relevant accretion rate is that in the external part of the accretion flow where wind mass-loss is negligible.

a small fraction can reach the vicinity of the accretor (see e.g. Pakull et al. 2006; Copperwheat et al. 2007). However, RSGs undergo a significant mass loss in stellar wind, which can be slow in the vicinity of the donor, therefore, can provide significant wind-fed mass transfer (MT) rate if the separation is small enough or the wind is focused towards the accretor (El Mellah et al. 2019). The presence of an accretion disk in at least two wind-fed XRBs was inferred from spectroscopic observations and modelling (Vela X-1, Liao et al. 2020; and Cyg X-1, Zdziarski 2014).

Recently, Heida et al. (2019) suggested, that the growing number of ULXs with RSG donor candidates prompts to reevaluate the significance of wind-driven MT in the context of ULXs. Up-to-date, no general population studies of wind-fed ULXs have been done, even though at least one ULX was detected with a donor that is not filling its RL (e.g. M 101 ULX-1, Liu et al. 2013). The aim of this article is to tackle this problem and, in particular, to answer the question: **how important is wind-fed accretion for ULX sources?** Specifically, we perform a **statistical analysis of binary evolution models** in the context of recent observations in order to derive the number and properties of wind-fed ULXs. In particular, **we focus on NS ULXs with RSG donors and progenitors of gravitational wave sources like GW170817.**

2. METHODS

Below we describe our adopted models (modes) of wind accretion. Inclusion of wind accretion in XRB models is the most significant difference in respect to the previous population studies of ULXs. Bondi-Hoyle-Lyttleton (BHL) accretion is a standard scheme of wind mass accretion in **StarTrack** (Belczynski et al. 2008, 2020). Additionally, we adapt **the wind RLOF (WRLOF) scheme**, that was already used by Iłkiewicz et al. (2019) to analyse the relation between SNIa and wide symbiotic stars.

2.1. Bondi-Hoyle-Lyttleton accretion

In the BHL scheme (Hoyle & Lyttleton 1939; Bondi 1952, for a recent review see Edgar 2004), we assume that the accretor is engulfed by a steady and uniform (at least in the vicinity of the accretor) supersonic wind from a companion star with $v_{\text{wind}} \gg v_{\text{orb}}$, where v_{wind} is the wind velocity relative to the accretor and v_{orb} is the orbital velocity of the accretor relative to the mass losing star. We calculate **the fraction of the wind mass-loss accreted by the compact body** as (for derivation see Belczynski et al. 2008, Equation 39)

$$\beta_{\text{acc,BHL}} = \frac{\dot{M}_{\text{acc,BHL}}}{\dot{M}_{\text{don,wind}}} = \frac{1}{\sqrt{1-e^2}} \times \left(\frac{GM_{\text{acc}}}{v_{\text{wind}}^2} \right)^2 \frac{\alpha_{\text{wind}}}{2a^2} \left(1 - \left(\frac{v_{\text{orb}}}{v_{\text{wind}}} \right)^2 \right)^{-\frac{3}{2}}, \quad (2)$$

where $\dot{M}_{\text{acc,BHL}}$ is the orbit-averaged wind accretion rate, e is the eccentricity, G is the gravitational constant, M_{acc} is the accretor's mass, a is the binary separation, and $\dot{M}_{\text{don,wind}}$ is the mass-loss rate in wind from the donor. α_{wind} is a numerical factor between 1–2 (Boffin & Jorissen 1988; Shima et al. 1985). Following Belczynski et al. (2008) we assume a conservative value of $\alpha_{\text{wind}} = 1.5$. We

impose a limit of $\dot{M}_{\text{acc,BHL}} \leq 0.8 \times \dot{M}_{\text{don,wind}}$ to avoid artificially high values resulting from orbital averaging. A formula similar to Equation 2 was first proposed by (Bondi 1952), but later Shima et al. (1985) showed that an additional factor of ~ 2 makes the Bondi's formalism fit their hydro-dynamical simulations and agree with the earlier simplified prescription of Hoyle & Lyttleton (1939).

Here we make an optimistic assumption that all the mass captured into the wake is consequently accreted, although only a fraction of this mass is expected to be accreted in a real situation (e.g. Edgar 2004). We also do not include any effects of orbital motion on the accretion flow which could additionally decrease the accretion rate (e.g. Theuns et al. 1996). Consequently, mass accretion rate calculated through Equation 2 should be perceived as an approximate upper limit and our results as optimistic.

2.2. Wind RLOF

When the stellar wind is slow inside the donor's RL, the assumption of wind isotropy may not be realistic, because the accretor can gravitationally focus the wind towards the L1 point, thus imitating RLOF-like mode of accretion (including formation of an accretion disk). In such a case one speaks about WRLOF. Mohamed & Podsiadlowski (2007) showed that in favourable circumstances it can provide much higher rates than BHL accretion. According to their simulations, which are limited to few special cases, **WRLOF MT rate can be even 100 times higher than for BHL.** The WRLOF has been already used to explain the observations of symbiotic stars (e.g., Mohamed & Podsiadlowski 2007; Iłkiewicz et al. 2019), carbon-enhanced metal-poor stars (Abate et al. 2013). Particularly, El Mellah et al. (2019) showed that in favourable conditions wind-powered XRBs with supergiant donors can appear as ULXs.

In detached binaries containing stars that have slow, dust-driven wind the MT may resemble the standard RLOF (Mohamed & Podsiadlowski 2007). The slow moving material fills the RL of the donor (stellar wind source), before being significantly accelerated by the radiation pressure and escaping preferentially through L1 point. Therefore a significant fraction of the wind may be collimated towards the orbital plane and the accretor.

The formalism for WRLOF used in the present study, which we describe below, was **first developed by** Abate et al. (2013). Motivated by numerical simulations (e.g. Mohamed 2010), we assume that the collimation of stellar wind toward the orbital plane and the accretor is significant when the radius where the stellar wind accelerated by the radiation pressure reaches **the escape velocity (R_d)** is comparable to or larger than the RL radius. Assuming $R_d \gg R_{\text{don}}$, the former can be approximated as (Höfner 2007):

$$R_d = \frac{1}{2} R_{\text{don}} \left(\frac{T_{\text{eff}}}{T_{\text{cond}}} \right)^{\frac{4p}{2}}, \quad (3)$$

where R_{don} is the donor's radius, T_{eff} the donor's effective temperature, T_{cond} is the condensation temperature of the dust, and p is a parameter. Although T_{cond} and p depend on the chemical composition, we assume the

values of $T_{\text{cond}} = 1500$ K and $p = 1$, which are consistent with properties of carbon-rich dust (e.g. Höfner 2007).

The stellar-wind fraction reaching the accretor is calculated as (Abate et al. 2013, see Equation 9 therein):

$$\beta_{\text{acc,WRLOF}} = \min \left\{ \left(\frac{q}{0.6} \right)^2 [c_1 x^2 + c_2 x + c_3], \beta_{\text{acc,max}} \right\}, \quad (4)$$

where $x = R_d/R_{\text{RL,don}}$, $R_{\text{RL,don}}$ is the RL radius of the donor, $c_1 = -0.284$, $c_2 = 0.918$, and $c_3 = -0.234$. $c_1 x^2 + c_2 x + c_3$ is a fit to the results of Mohamed (2010) made for $q = 0.6$, q being the mass ratio (donor mass over accretor mass). $(q/0.6)^2$ is the scaling proposed by Abate et al. (2013) to account for the influence of the mass ratio on the MT rate. $\beta_{\text{acc,max}} = 0.5$ is the highest value of β_{acc} obtained by Mohamed (2010), which we use as the limit for all values of q . If the MT rate calculated for the WRLOF is higher than the BHL rate, we assume that MT occurs through WRLOF mode. In the opposite case, we assume that it occurs through BHL mode.

We are aware that the simulation of Mohamed (2010) and calculations by Abate et al. (2013) were performed for a narrow region of the parameter space (viz. specific values of accretor and donor masses). Nonetheless, we extended the applicability of their results to suit the needs of population synthesis calculations. In our reference model (WM8), we allow for the WRLOF MT mode only from donors less massive than $8 M_{\odot}$, which is just the maximal mass to which simulations were performed in Mohamed (2010). For comparison we provide also the results for two other models. In the WM0 model the WRLOF MT is not possible and all wind-fed systems transfer mass using BHL mode. On the other hand, in the model WM+, WRLOF MT is allowed for all donors irrespective of their mass. These two variations may be seen as extreme cases as far as the importance of WRLOF is concerned.

The standard model for stellar winds as implemented in *StarTrack* is described in Belczynski et al. (2010a). In short, we use the wind mass-loss prescriptions for OB stars based on observational data (Vink et al. 2001; Vink 2008). For Wolf-Rayet wind the code accounts for clumping (Hamann & Koesterke 1998) and metallicity dependence (Vink & de Koter 2005). Wind mass-loss rates for luminous blue variable stars are calculated from $1.5 \times 10^{-4} (M/M_{\odot}) M_{\odot} \text{ yr}^{-1}$ (Vink & de Koter 2002; Belczynski et al. 2010a). For low-mass stars we follow the formalism of Hurley et al. (2000).

2.3. Simulations

In order to obtain statistically significant comparison of observational data on ULX sources with models of wind-fed accretion, we utilized the population synthesis code *StarTrack* (Belczynski et al. 2008, 2020). In the previous paper (Wiktorowicz et al. 2019a) we have analyzed the observed population of ULXs, but focused on the RLOF systems only. In the current work, ULXs in which accretion occurs via RLOF serve as a reference point. The beaming, i.e. anisotropic emission of radiation, can be present in ULXs in general (e.g. Wiktorowicz et al. 2019a) and, specifically, in PULXs (King & Lasota 2020). Therefore, we include these effect in our analysis of wind-fed ULXs as was previously done for the population of RLOF ULXs in Wiktorowicz et al. (2019a).

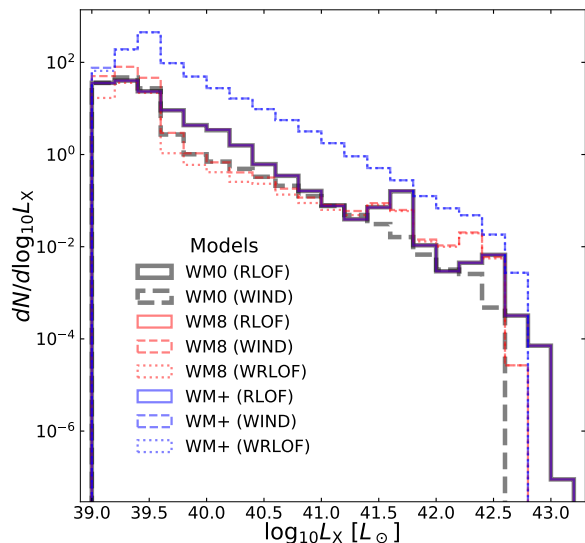


FIG. 1.— Distributions of X-ray luminosity (L_X) of ULXs for various models tested in this study (see text for details). Designations in parenthesis mark the ULX subpopulations: RLOF-powered by the RLOF accretion mode; WIND-powered by wind-fed accretion (both WRLOF and BHL modes); WRLOF-powered by WRLOF accretion mode only.

In order to compare the theoretical binary evolution models and observational data, we calculate the predicted number of RLOF-fed and wind-fed ULXs, for a fiducial galaxy that is to resemble the Milky Way. Specifically, we assumed the total stellar mass to be $M_{\text{tot}} = 6.08 \times 10^{10} M_{\odot}$ (Licquia & Newman 2015), a uniform metallicity distribution ($Z = Z_{\odot} = 0.02$) and constant star formation rate (SFR) throughout the last 10 Gyr equal to $6.08 M_{\odot} \text{ yr}^{-1}$. We present also results for burst-like star formation episodes ($\Delta t = 100$ Myr; $\text{SFR} = 608 M_{\odot} \text{ yr}^{-1}$) for comparison at two moments: 100 Myr and 2 Gyr after the commencement of star formation (i.e. right after and 1.9 Gyr after the star formation ceases), which correspond to young and old stellar populations respectively. Due to the inaccuracies of evolutionary models and sparse observational data, no more-detailed Galactic model is necessary in the context of this work.

3. RESULTS

3.1. Observable sample

Table 1 presents the abundance of ULXs (both RLOF- and wind-fed) in our results. Although these numbers are rather optimistic due to favorable assumption, particularly, the high recent SFR used in the simulations and the omission of interstellar absorption, they show that the inclusion of wind-fed sources in ULX populations studies is necessary. Wind-fed ULXs may not only represent a significant fraction of the ULX population (e.g. 49–89% for constant star formation history) but, in favorable conditions (e.g. very young stellar environments), be its dominant component.

The population of ULXs is dominated by sources with low luminosities ($\lesssim 3 \times 10^{39} \text{ erg s}^{-1}$) both for RLOF and

TABLE 1
NUMBER OF ULXS FOR A FIDUCIAL GALAXY

Model	Constant SF			Burst SF (100 Myr ago)			Burst SF (2 Gyr ago)		
	RLOF	WIND	f_{WRLOF}	RLOF	WIND	f_{WRLOF}	RLOF	WIND	f_{WRLOF}
All Companions									
WM0	2.4×10^1	2.3×10^1	—	6.8×10^2	2.1×10^3	—	2.2×10^1	3.7×10^{-2}	—
WM8	2.4×10^1	3.7×10^1	42.50%	6.8×10^2	2.9×10^3	33.63%	2.2×10^1	1.7×10^{-2}	100.00%
WM+	2.4×10^1	1.9×10^2	97.24%	6.8×10^2	1.8×10^4	97.96%	2.2×10^1	1.7×10^{-2}	100.00%
Supergiant Companions									
WM0	5.3×10^{-2}	2.0×10^1	—	5.2	1.8×10^3	—	—	—	—
WM8	5.3×10^{-2}	3.3×10^1	44.45%	5.2	2.7×10^3	36.08%	—	—	—
WM+	5.3×10^{-2}	1.8×10^2	98.60%	5.2	1.8×10^4	99.33%	—	—	—
RSG companions									
WM0	1.6×10^{-5}	2.0×10^1	—	1.6×10^{-3}	1.8×10^3	—	—	—	—
WM8	1.6×10^{-5}	3.2×10^1	43.51%	1.6×10^{-3}	2.6×10^3	35.57%	—	—	—
WM+	1.6×10^{-5}	1.8×10^2	98.56%	1.6×10^{-3}	1.7×10^4	99.32%	—	—	—

NOTE. — Predicted numbers of ULXs powered by Roche lobe overflow (RLOF) and wind accretion (WIND) in a fiducial galaxy (see text for details). f_{WRLOF} gives a fraction of wind-fed ULXs in which MT occurs through wind RLOF mode (Section 2.2). Models presented are: WM0 in which only BHL accretion mode is possible, WM8 in which WRLOF accretion mode possible, but limited to donors lighter than $8 M_{\odot}$, and WM+ in which WRLOF accretion mode possible for donors of all masses. Additionally, supergiant and RSG donors are shown separately. Supergiant companions are defined as post-MS stars with luminosity $L > 15000 L_{\odot}$ and surface gravity $\log g < 2$, whereas RSGs, a subpopulation of supergiants, additionally have effective surface temperatures lower than 4kK. Results for three reference SFHs are presented: constant through 10 Gyr and burst-like with a duration of 100 Myr which started 100 Myr or 2 Gyr ago. Zeros are marked with ‘—’ for clarity.

wind-powered sources (Figure 1). These are mainly BH ULXs emitting isotropically and mildly-beamed (beaming factor³ $b \gtrsim 0.2$) NS ULXs. In the case of wind-fed ULXs, both modes (viz. BHL and WRLOF) are possible. As far as the most luminous sources are concerned, the highest luminosities (up to $\sim 10^{43} \text{ erg s}^{-1}$) are obtained for binaries consisting of a NS with a Helium rich donor or a BH with a HG donor (see also Wiktorowicz et al. 2015). In the case of wind-fed sources, these highly luminous group is composed of ULXs with BH accretors transferring mass through the WRLOF mode exclusively. In all cases, we assume that the beaming is saturated at $b \approx b_{\text{min}} = 3.2 \times 10^{-3}$ (Lasota et al. 2016; Wiktorowicz et al. 2017). We note, that no ULXs have been observed with luminosities much above $\sim 10^{42} \text{ erg s}^{-1}$ and some ULXs with luminosities above $\sim 10^{41} \text{ erg s}^{-1}$ might actually contain intermediate-mass BHs (e.g. Greene et al. 2019), which are not included in our study. Nonetheless, such luminous stellar-mass ULXs are rare (we predict $\sim 10^{-7}$ per Milky Way equivalent galaxy), but may exist undetected in distant galaxies. King (2009) suggested that such highly beamed and apparently luminous sources may mimic distant AGNs acting as “pseudoblazars.”

The wind-fed ULXs can reach similar luminosities as RLOF systems despite the large fraction of mass being lost from the system (e.g. Mohamed 2010, obtained that no more than 50% of wind is accreted). This is possible, because the wind-fed systems do not suffer from the dynamical instability when the mass ratio is high ($\gtrsim 3$), even when their envelopes are convective (van den Heuvel et al. 2017, and references therein), and can have very massive donors. Consequently, progenitors of wind-fed ULXs are typically more massive on the ZAMS and

have larger separations to accomodate expanding stars (Figure 2).

The RLOF powered ULXs typically have much longer duration of the emission phase ($> 5 \text{ Myr}$) than wind-fed systems ($\sim 1 \text{ Myr}$ for WRLOF and $\sim 0.1 \text{ Myr}$ for BHL; see Figure 3). The donors in wind-fed systems are typically massive stars (Figure 7) in short-lived supergiant phase (e.g. $\sim 1.5 \text{ Myr}$ for $5 M_{\odot}$ asymptotic giant branch star (AGB) or $\sim 0.1 \text{ Myr}$ for $10 M_{\odot}$ AGB star) when their wind is relatively slow and dense. On the other hand, RLOF accretion may give high MT rates even for low-mass companions at the end of MS phase (e.g. Wiktorowicz et al. 2017). Low-mass stars have significantly longer life spans than their heavier cousins, therefore, potentially longer MT phases and less often enter dynamical-time MT when their RL is filled. We note that, only in rare situations it is possible that the donor in a RLOF-powered ULX fills its RL immediately after the compact object formation as a result of favorably directed natal kick (see e.g. Maxted et al. 2020), so that its MT phase can be the longest possible. In a typical case, the RL is filled only after the star expands as a result of nuclear evolution, typically shortly ($\lesssim 100 \text{ Myr}$) before TAMS.

RLOF ULXs are typically associated with low- and medium-mass donors ($\lesssim 10 M_{\odot}$), whereas wind-fed ones typically have massive donors ($\gtrsim 10 M_{\odot}$; Figure 7). Although low-mass stars are more abundant among primaries due to the shape of the initial mass function ($\Gamma < 0$), flat initial mass ratio distribution makes massive companions more prevalent among NS/BH progenitors (Figure 2; see also Wiktorowicz et al. 2019b). This situation favors wind-fed ULXs. The higher the mass of a star, the stronger is the mass loss in stellar wind for a particular evolutionary phase, what makes a binary with compact object progenitor and massive secondary a perfect predecessor of a wind-fed ULX. Moreover, when a massive star fills its RL after the primary forms a compact object, the mass ratio may be too high to provide

³ The beaming factor b is the ratio of the solid angle of emission and the whole sphere. In this study we assume $b = \min(1, 73/(\dot{M}/\dot{M}_{\text{Edd}})^2)$, where \dot{M} and \dot{M}_{Edd} are the actual and the Eddington accretion rates, respectively (King 2009; Wiktorowicz et al. 2019a).

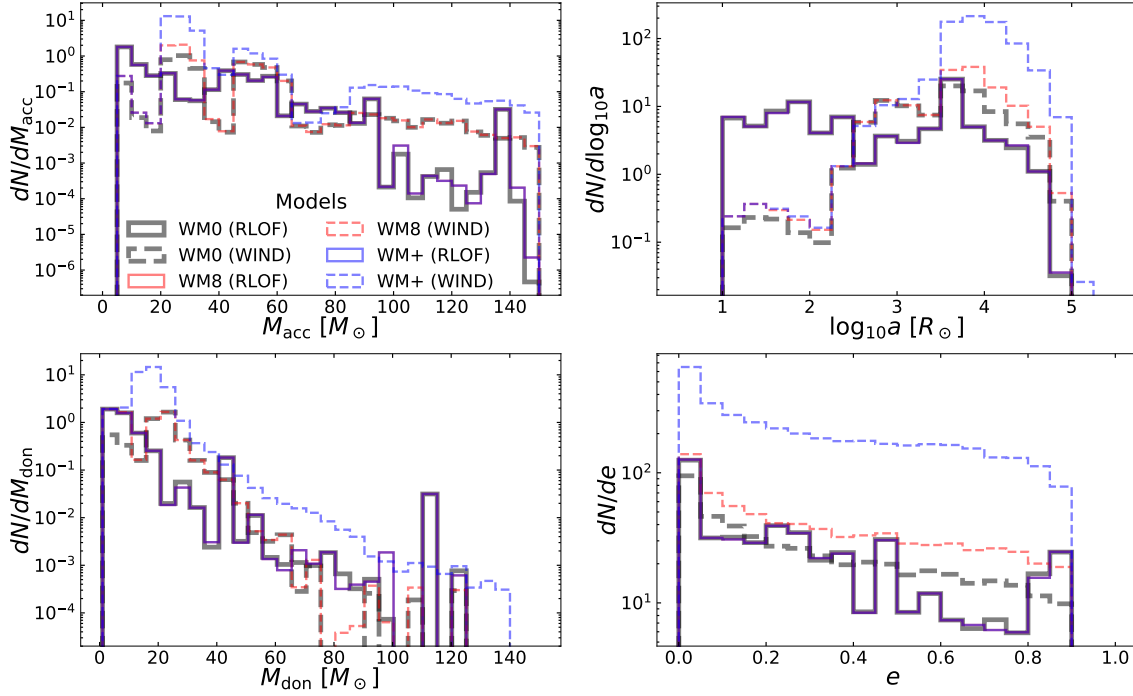


FIG. 2.— Initial distributions of parameters for ULX progenitors with division on different tested models and accretion modes (see caption of Figure 1). Parameters are: M_{acc} —accretor mass; M_{don} —donor mass; a —separation; e —eccentricity.

ies (e.g. Wiktorowicz et al. 2017).

3.2. Typical evolution

Wind-fed ULXs are expected to comprise a large fraction (up to $\sim 96\%$) of ULXs in star-forming environments, but practically disappear ($< 1\%$) in old environments (Table 1). These systems may contain either a BH or a NS accretor and be powered by WRLOF or BHL wind accretion mode, however, in older environments ($\gtrsim 1$ Gyr after the end of star-formation) NS accreting through WRLOF mode dominate the population. Below, we compare various evolutionary routes leading to the formation of wind-fed ULXs and their posterior evolution.

The most common wind-fed ULXs are those with NS accretors and MT occurring through the WRLOF mode. Donors in these systems are typically low-mass ($0.7\text{--}2.6 M_{\odot}$) AGB stars. In a typical case (Figure 4, upper plot), the binary on ZAMS composes of a $7.48 M_{\odot}$ primary and a $2.28 M_{\odot}$ secondary on a medium-size orbit of $\sim 3200 R_{\odot}$ with moderate eccentricity ($e \approx 0.2$). The primary evolves and becomes an AGB star at the age of 48 Myr. The stellar wind leads to a significant mass loss, part of which is being captured by the secondary. Finally, the primary becomes a $1.36 M_{\odot}$ ONe white dwarf (WD), whereas the secondary grows to $\sim 3 M_{\odot}$ while still being on the MS. After 460 Myr the secondary evolves off the MS and becomes an AGB star what results in a significant rise in the rate of mass loss in stellar wind. The WD captures a fraction of the wind, what allows it to grow to $1.38 M_{\odot}$, when the accretion induced collapse trans-

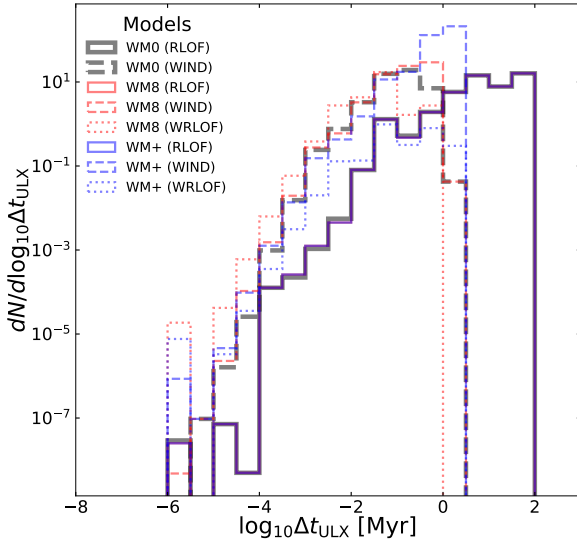


FIG. 3.— Distribution of the ULX phase total duration times (Δt_{ULX}) with a division on different models and accretion modes (see the caption of Figure 1). When a system has more than one ULX phase during its evolution, durations are combined.

a stable RLOF MT and instead a CE occurs barring the formation of a ULX. We note, that ULXs powered by RLOF MT were discussed thoroughly in previous stud-

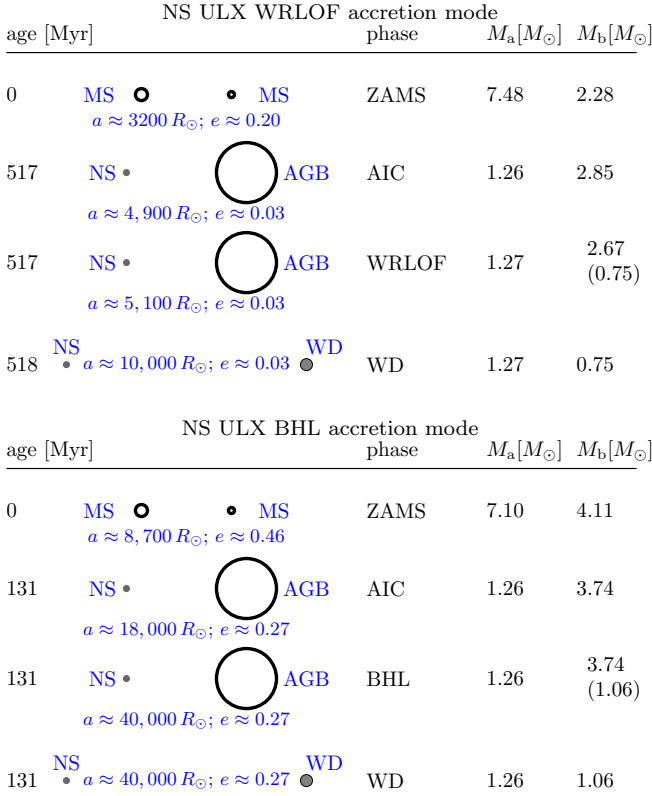


FIG. 4.— Symbolical representation of a typical system evolution leading to the formation of wind-fed NS ULXs. Upper/Lower plots show routes with WRLOF/BHL accretion mode. The columns represent the age of the system, scheme of the system (not to scale), evolutionary phase, and masses of the primary and secondary. The binary evolution phases are as follows: ZAMS—zero age main sequence; AIC—accretion induced collapse; WRLOF—phase of wind accretion through WRLOF mode; BHL—phase of wind accretion through Bondi-Hoyle-Lyttleton mode; WD—white dwarf formation. Additionally, the schemes present separations (a), eccentricities (e), and stellar evolutionary phases: MS—main sequence; AGB—asymptotic giant branch; NS—neutron star; WD—white dwarf.

forms it into a $1.26 M_\odot$ NS. The secondary remains an AGB star for the next 0.7 Myr, while the mass loss increase and in a short time reaches $\sim 10^{-6} M_\odot \text{ yr}^{-1}$ out of which 37% is captured into the primary disk which marks the beginning of the ULX phase. It lasts for 100 kyr and the luminosity reaches $\sim 4 \times 10^{41} \text{ erg s}^{-1}$. Afterwards, the secondary becomes a $0.75 M_\odot$ CO WD.

The progenitors of NS ULXs powered through the BHL mode require heavier companions ($1.2\text{--}2.4 M_\odot$) and larger initial separations. In a typical case (Figure 4, lower plot) the system consist, initially, of a $7.1 M_\odot$ primary and $4.1 M_\odot$ secondary on a wide eccentric orbit ($a \approx 8700 R_\odot$; $e \approx 0.46$). The primary, while ascending the AGB, loses most of its mass and at the age of 54 Myr becomes an ONe WD. As a result of mass accretion the secondary grows to $\sim 5.5 M_\odot$ and after 80 Myr becomes an AGB star. In one Myr it loses nearly $2 M_\odot$ of its mass, due to strong stellar wind, a fraction of which is captured by the WD, which increases its mass to $1.38 M_\odot$ when the electron-capture SN results in the formation of a NS. In such an accretion induced collapse, the natal kick is expected to be low, which allows the wide binary with a separation of $18,000 R_\odot$ and moderate eccentricity of $e \approx 0.27$ to survive. Such a large separation makes WRLOF ineffective and the MT occurs through

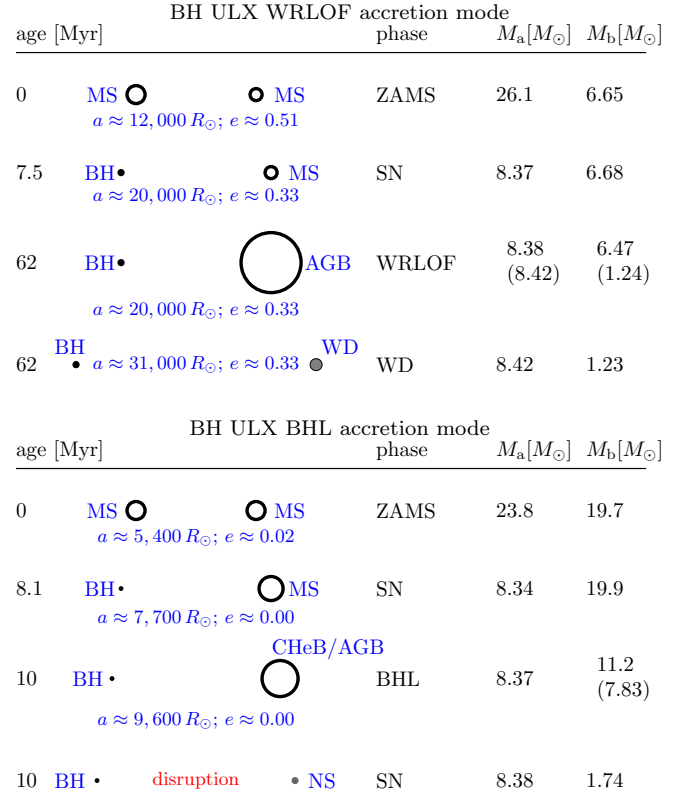


FIG. 5.— Same as Figure 4, but for ULXs with BH accretors. Additional abbreviations (not present in Figure 4) for binary evolution include: SN—supernova, i.e. formation of the compact object; whereas for stellar evolution: BH—black hole; CHyB—core Helium burning.

the BHL mode. Although the fraction of the wind being accreted is small ($\sim 2\%$), the strong stellar wind ($6.5 \times 10^{-5} M_\odot \text{ yr}^{-1}$) makes the effective MT quite high ($1.5 \times 10^{-6} M_\odot \text{ yr}^{-1}$), comparable to that in typical NS ULX powered through the WRLOF mode (see paragraph above). The luminosity reaches 3.5×10^{40} for a brief moment, but within 3 kyr the system dims and becomes a regular XRB. After 100 kyr, the secondary becomes a WD with a mass of $\sim 1.06 M_\odot$.

We note that AGB stars with mass-loss rates as in the above examples are observed in the Large Magellanic Cloud (e.g. Höfner & Olofsson 2018). Therefore, accretion efficiencies in WRLOF mode necessary to power a ULX for the observed mass-loss rates are within the model range (i.e. ≤ 0.5). Concerning the BHL accretion mode, we may estimate the accretion radius as $R_{\text{acc}} = 2GM_{\text{acc}}/v_{\text{inf}}^2$, where G is the gravitational constant and v_{inf} is the terminal wind velocity (e.g. Edgar 2004). The fraction of accreted wind may be further estimated as the fraction of the wind which falls within the accretion radius: $f_{\text{acc}} = 0.5 \sin R_{\text{acc}}/a \approx 0.095 (M/M_\odot)(v_{\text{inf}}/10 \text{ km s}^{-1})^{-2}(a/20,000 R_\odot)^{-1}$, where $v_{\text{inf}} \approx 10 \text{ km s}^{-1}$ is the typical value for AGB stars (e.g. Höfner & Olofsson 2018). Although these estimations are very rough (see Section 4.2), they show that the MT rates in the typical routes are feasible.

The companions in wind-powered BH ULXs are in general more massive than in NS ULXs, what results from the fact that heavier primaries (BH progenitors) are typically accompanied by heavier secondaries ($\gtrsim 10 M_\odot$)

on the ZAMS (e.g. Wiktorowicz et al. 2019b). For BH ULXs, in which the MT occurs through WRLOF mode, the typical companion mass is $5\text{--}7\text{ M}_\odot$, whereas a BH is typically $\sim 8\text{--}9\text{ M}_\odot$. In a typical evolution leading to the formation of such a system (Figure 5, upper plot), the primary on ZAMS is 26.1 M_\odot , whereas the secondary is 6.65 M_\odot , and the separation is $12,000\text{ R}_\odot$ with significant eccentricity $e \approx 0.51$. The primary evolves faster and after 6.7 Myr becomes a CHeB star. A high wind mass-loss starts that decreases the star’s mass to 9.2 M_\odot in just 700 kyr. A fraction of this mass is accreted by the secondary, which allows it to remain its initial mass of $\sim 6.7\text{ M}_\odot$ despite losses in stellar wind. Shortly after, the primary forms a 8.37 M_\odot BH. Meanwhile, the separation increases to 20000 R_\odot and the eccentricity changes to 0.33. The secondary needs more than 50 Myr to evolve off the MS and become an AGB star, when its wind mass loss grows significantly to 4.6×10^{-7} . The wind is still slow inside the RL, therefore, a large fraction ($\sim 50\%$) is gravitationally collimated towards the L1 point and feeds the accretion disk of the primary. For 500 kyr the MT through WRLOF mode is high enough to power a ULX with the peak luminosity reaching $\sim 10^{42}\text{ erg s}^{-1}$. Afterwards, the secondary becomes a CO WD with a mass of 1.23 M_\odot .

The evolution leading to the formation of BH ULXs powered by BHL accretion (Figure 5, lower plot) differs significantly from the cases described above. The companions are significantly more massive, $9\text{--}12\text{ M}_\odot$, thus the WRLOF can operate only in WM+ model, which allows for wind collimation from donors with masses above 8 M_\odot . On the ZAMS, the binary consists of a 23.8 M_\odot primary and a 19.7 M_\odot secondary on an orbit of $5,400\text{ R}_\odot$, which is nearly circular ($e \approx 0.02$). The primary evolves and in 7.3 Myr becomes a CHeB star, which commences a significant mass loss in stellar wind. Within 800 kyr the star loses more than half of its mass in stellar wind and becomes a 8.34 M_\odot BHs. The secondary evolves and at the age of $\sim 10\text{ Myr}$, as a CHeB star, provides a MT rate of $1.2 \times 10^{-5}\text{ M}_\odot\text{ yr}^{-1}$ out of which $\sim 2\%$ reaches the vicinity of the accretor. It is high enough to power an isotropic ULX ($L_X \approx (2\text{--}3) \times 10^{39}\text{ erg s}^{-1}$) for $\sim 100\text{ kyr}$. Meanwhile, the secondary evolves into an AGB star and the luminosity of the ULX increases to reach $\sim 10^{42}\text{ erg s}^{-1}$. After that time, the secondary, having a mass of 7.8 M_\odot , undergoes a SN and becomes a NS. However, the NS’s natal kick on such a wide orbit ($a \approx 13,000\text{ R}_\odot$) results in a binary disruption. We note that the accretion mode in this scenario is forced by the limit on the maximal mass of donor as 8 M_\odot in WRLOF mode for the reference mode. In WM+ model, this ULXs will transfer mass through WRLOF mode, but the peak luminosity will be similar.

A few ULXs evolve through both the RLOF powered phase and wind powered phases. This situation occurs for 4% of RLOF ULXs and 5% of wind-fed ULXs (1%/8% in the case of WM0/+ models, respectively) predicted to be observed currently in the modeled galaxy. In a typical case (Figure 6, such a binary on the ZAMS is composed of a 29.9 M_\odot primary and 3.56 M_\odot secondary, whereas the separation and eccentricity are 4400 R_\odot and 0.10, respectively. The primary evolves much faster and becomes a CHeB star. The mass loss in the stellar wind removes most of the hydrogen envelope, so when the star fills its











age [Myr]		phase	$M_a[M_\odot]$	$M_b[M_\odot]$
0	MS   MS $a \approx 4,400\text{ R}_\odot; e \approx 0.10$	ZAMS	29.9	3.56
6.7	BH   MS $a \approx 120\text{ R}_\odot; e \approx 0.01$	SN	8.45	3.59
240	BH   RG $a \approx 120\text{ R}_\odot; e \approx 0.00$	RLOF	8.45 (8.59)	3.59 (0.96)
290	BH   AGB $a \approx 1,200\text{ R}_\odot; e \approx 0.00$	BHL	8.59 (8.60)	0.96 (0.81)
290	BH   WD $a \approx 1,700\text{ R}_\odot; e \approx 0.00$	WD	8.60	0.79

FIG. 6.— Same as Figure 4, but for a ULX that is powered first by RLOF accretion and later by wind accretion. Additional abbreviations (not present in Figures 4 and 5) for the binary evolution are: RLOF—Roche-lobe overflow; and for stellar evolution: RG—red giant.

RL at the age of 6.5 Myr the companion easily rejects the CE and the separation shrinks to 100 R_\odot . The primary evolves as a helium star for 200 kyr and forms a 8.45 M_\odot BH. The orbit now is close enough for the secondary expanding as a RG to fill its RL and start a RLOF, which is strong enough to power a ULX and lasts for 400 kyr with a luminosity of approximately $6 \times 10^{39}\text{ erg s}^{-1}$. The secondary detaches as the separation grows to 280 R_\odot . Its RL is filled again when the star ascends the AGB. When the separation grows to $1,200\text{ R}_\odot$ the star detaches, but still nearly fills its RL resulting in significant MT rate through WRLOF mode that powers a ULX for 100 kyr with a luminosity of $\sim 3 \times 10^{39}\text{ erg s}^{-1}$. Afterwards, the secondary forms a 0.79 M_\odot WD.

3.3. Donors

Figure 7 presents the parameter distributions of donors in the sample of wind-fed ULXs. Donors in RLOF ULXs were thoroughly investigated in our previous papers (e.g. Wiktorowicz et al. 2017) and are provided here only for reference.

Masses of donors in wind-fed systems are on average larger than in RLOF-fed ones and reach 30 M_\odot for WM0/8 models, or $\sim 70\text{ M}_\odot$ for WM+ model. Wind-fed accretion does not suffer from dynamical instability for high mass-ratio systems, which is the case of RLOF stars with convective envelopes, and allows for $q \gtrsim 3$. On the other hand, the heavier the star, the shorter is its lifetime, which significantly limits the estimated number of ULXs with most massive donors and localizes them in star-forming regions or their immediate vicinity.

The evolutionary stage of wind-feeding donors is markedly different from those in RLOF ULXs, which are predominantly MS and He-rich stars. In wind-fed ULXs these are mostly CHeB and AGB stars that have significantly expanded due to nuclear evolution and produce dense and slow stellar wind. Being more massive, donors in wind-fed systems are also on average much younger than in RLOF ULXs. However, those in orbit with NSs may be much older and the ULX phase can occur as late as $> 1\text{ Gyr}$ after the ZAMS. We note, that in a typical situation, the secondary becomes rejuvenated while ac-

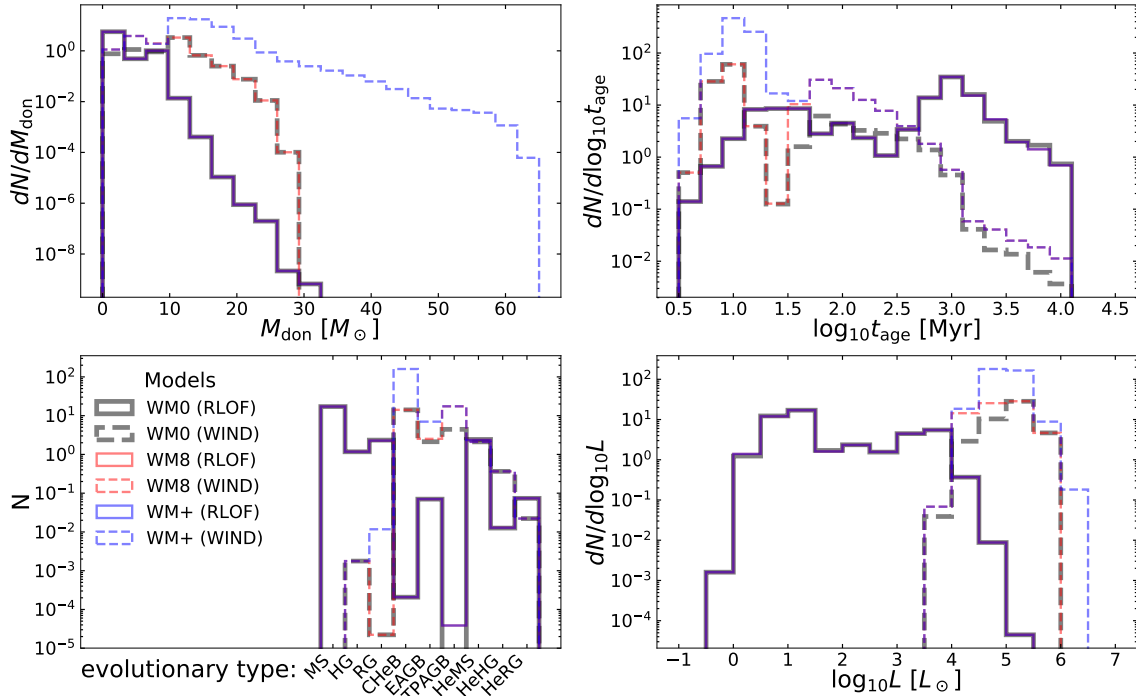


FIG. 7.— Distributions of ULX donor parameters: mass (M_{comp} , upper-left), age since ZAMS at the moment of observation (t_{age} , upper-right), evolutionary type (lower-left), and bolometric luminosity (L , lower-right). The maximal age of the ULXs was limited to 10 Gyr due to the duration of the simulation. Model names and accretion modes are defined in caption to Figure 1. Evolutionary types are: MS—main sequence; HG—Hertzsprung gap; RG—red giant; CHeB—Core Helium burning; EAGB—early asymptotic giant branch; TPAGB—thermal pulsing asymptotic giant branch; HeMS—Helium main sequence; HeHG—Helium Hertzsprung gap; HeRG—Helium red giant.

creting from stellar wind blown out from the evolving primary.

Donors in wind-fed ULXs are also more luminous than those in RLOF systems, mainly because of their higher masses and advanced evolutionary phase, with luminosities reaching $\sim 10^6 L_{\odot}$. Such luminosities should be easily detectable at extra-galactic distances, where the majority of ULXs are observed, and agrees with the fact that most of the donor candidates in ULXs are RSGs (Heida et al. 2019).

In studies of ULX populations, RSG donors composed a minority (e.g. $\lesssim 1\%$ in Wiktorowicz et al. 2017) as we show also in this study ($\sim 6.8 \times 10^{-5}\%$). It didn't produce a conflict with observations, because donor candidates were detected only in a handful of ULXs and the observations were strongly biased toward detection of NIR objects. Additionally, ULXs are predominantly extra-galactic objects, so low-mass, and therefore dim, stars, which theoretically dominate donors in RLOF-fed ULXs (e.g. Wiktorowicz et al. 2017), are naturally excluded from detection. However, our study of wind-fed ULXs shows that in reality RSG might compose a significant fraction of ULXs and in particular dominate those which are wind-fed ($\gtrsim 88\%$; see Table 2). In particular, $\gtrsim 36\%$ of them may transfer mass through the WRLOF mode. Only in old stellar environments ($t_{\text{age}} \gtrsim 1$ Gyr) the fraction of RSGs among ULXs peters out (Table 1) due to their short lifetimes. Noteworthy, none of the

ULXs with RSG donors will evolve into a merging DCO (Section 3.4) and; instead, they will typically form wide systems composed of a compact object and a carbon-oxygen WD.

According to our results, RSGs are expected to dominate the populations of wind-fed ULXs. This abundance of RSGs in our sample of synthetic ULXs suggests that the apparent connection between ULXs and RSGs in the observational data might be real.

3.4. Double Compact Object Progenitors

ULXs are among the potential double compact object (DCO) progenitors (e.g. Mondal et al. 2020). Heida et al. (2019) suggested that especially ULXs harboring RSGs, thus massive stars, are good candidates. However, as we have shown in Section 3.2, the majority of ULXs with RSG donors (and wind-fed ULXs in general) are expected to form either wide BH/NS-WD binaries, or be disrupted. In this section we analyse the evolutionary routes leading to the formation of DCOs from wind-fed ULXs with a particular attention put on merging ones (mDCOs; i.e. with time to merger, $t_{\text{merge}} < 10$ Gyr).

Up to 46% of wind-fed ULXs (depending on the model) will form DCOs. Much fewer (up to 6%) represent progenitors of mDCOs (Table 2). Although the fractions of mDCO progenitors for tested models are different, all predict similar expected number of these systems (about 1.4 per Milky Way-like galaxy), because all of them are

TABLE 2
DOUBLE COMPACT OBJECT PROGENITORS AMONG ULXs

Model	MT mode		All	DCO	mDCO	WRLOF DCO
WM0	RLOF	all	2.4×10^1	$7.2 \times 10^{-3}\%$	$1.1 \times 10^{-3}\%$	—
		RSG	$6.8 \times 10^{-5}\%$	$1.7 \times 10^{-5}\%$	—	—
	WIND	all	2.3×10^1	46%	6.0%	—
		RSG	88%	39%	—	—
WM8	RLOF	all	2.4×10^1	$7.2 \times 10^{-3}\%$	$1.1 \times 10^{-3}\%$	—
		RSG	$6.8 \times 10^{-5}\%$	$1.7 \times 10^{-5}\%$	—	—
	WIND	all	3.7×10^1	32%	3.8%	3.2%
		RSG	89%	27%	—	3.0%
WM+	RLOF	all	2.4×10^1	$7.2 \times 10^{-3}\%$	$1.1 \times 10^{-3}\%$	—
		RSG	$6.8 \times 10^{-5}\%$	$1.7 \times 10^{-5}\%$	—	—
	WIND	all	1.9×10^2	15%	0.75%	14%
		RSG	95%	14%	—	14%

NOTE. — Predicted number of all ULXs for the tested models and accretion modes (see caption of Table 1) with fractions of this number that fall into different categories: All—all systems; DCO—ULXs that are DCO progenitors; mDCO—ULXs that are progenitors of merging DCOs; WRLOF DCO—ULXs that transfer mass through WRLOF mode and are DCO progenitors. Calculated for a Milky Way-like galaxy with constant star-formation history. Rows labeled “RSG” present the sub-population of ULXs with RSG donors. There are no ULXs that are progenitors or merging DCOs and transfer mass through WRLOF mode. Zeros are marked as “—” for clarity.

nearly exclusively powered through the BHL accretion mode and none through WRLOF, the prescription for which presents the only difference between models. We note that nearly all ($\gtrsim 99\%$) of mDCO progenitors are wind-fed systems. Wind-powered systems can have much heavier donors ($M_{\text{ZAMS}} \gtrsim 8 M_{\odot}$; thus progenitors of compact objects), because the high mass-ratio ($\gtrsim 3$) does not lead to CE, which is an expected outcome if the RL is filled.

The small fraction of mDCO progenitors among ULXs results mainly from the preference for NS-forming donors in these systems⁴ and the resulting disruption of the system (due to the natal kick). Even if such a system survives supernova explosion without being disrupted, or it has evolved without a RLOF/CE phase, it will be on average too wide for a merger to occur within 10 Gyr, i.e. $t_{\text{merger}} > 10 \text{ Gyr}$.

The properties of mDCO progenitors are presented in Figure 8. The x-axis ranges were left the same as in the similar plots for the general distributions (Figure 7), so several distinct features are visible. Specifically, accretors are mostly BHs with a typical mass of $8\text{--}10 M_{\odot}$, whereas donors are evolved Helium-rich stars with a typical mass of $5\text{--}7 M_{\odot}$ and very high luminosities ($\log_{10} L/L_{\odot} \approx 5$). These ULXs are typically very young objects with $t_{\text{age}} \ll 100 \text{ Myr}$, so expected only in star-forming environments. Massive primaries and short orbital periods make the survival of the second SN more viable, but still most of these systems are disrupted (e.g. Wiktorowicz et al. 2019b).

⁴ Companion stars in ULXs are typically secondaries (e.g. Wiktorowicz et al. 2017), i.e. less-massive stars on ZAMS. For a uniform mass ratio distribution, the secondaries mass is typically half the mass of the primary. Therefore, if the secondary is to have an initial mass larger than $\sim 20 M_{\odot}$, i.e. the lower limit for BH formation in isolation, the primary should have typically the initial mass larger than about $40 M_{\odot}$. Due to the steepness of the IMF, such primary masses are rare.

Progenitors of mDCOs among wind-fed ULXs are mainly composed of a BH accretor with $8\text{--}9 M_{\odot}$ and a $5\text{--}7 M_{\odot}$ evolved star that transfers mass through BHL mode. As said above, there are no mDCO progenitors among ULXs powered through WRLOF mode as these are expanded post-MS stars on wide orbits and evolve typically into wide binaries with $t_{\text{merge}} \gg 10 \text{ Gyr}$. In a typical case of a mDCO progenitor (Figure 9), both stars are initially relatively massive ($49.0 M_{\odot}$ and $21.6 M_{\odot}$), the separation is moderate ($a \approx 380 R_{\odot}$), and the orbit is nearly circular ($e \approx 0.03$). In about 4.4 Myr primary evolves off the MS and commences a MT onto the secondary, which leads to a mass reversal. In the next half Myr, the primary forms a BH with a mass of $8.14 M_{\odot}$, while the orbit expands to $1,800 R_{\odot}$. The secondary needs additional $\sim 3 \text{ Myr}$ to become a giant and fill its RL starting the CE phase, which results in a significant shrinkage of the separation (down to about $4.1 R_{\odot}$). Being ripped off its hydrogen layers, the secondary becomes a Helium MS star with the stellar wind strong enough to power a ULX though a BHL mode (MT rate of $1.8 \times 10^{-6} M_{\odot} \text{ yr}^{-1}$ out of which $\sim 15\%$ is transferred to the vicinity of the BH, which is enough to power an isotropic ULX). After about 0.7 Myr it fills its RL and the MT mode switches to RLOF, which is much stronger and powers a hyper ULX (MT rate of $1.3 \times 10^{-3} M_{\odot} \text{ yr}^{-1}$ and luminosity of $L_{\text{X}} \approx 10^{42} \text{ erg s}^{-1}$). In a very short time (800 yr), the secondary explodes as a SN and forms a NS. The natal kick alters the orbit to a separation of $9.1 R_{\odot}$ and eccentricity of $e \approx 0.24$. The time to merger is $t_{\text{merge}} = 25.2 \text{ Myr}$.

4. DISCUSSION

4.1. Observed Systems

Although hundreds of ULXs have been detected so far (e.g. Walton et al. 2011; Swartz et al. 2011), only a handful of them has viable donor candidates. The observed

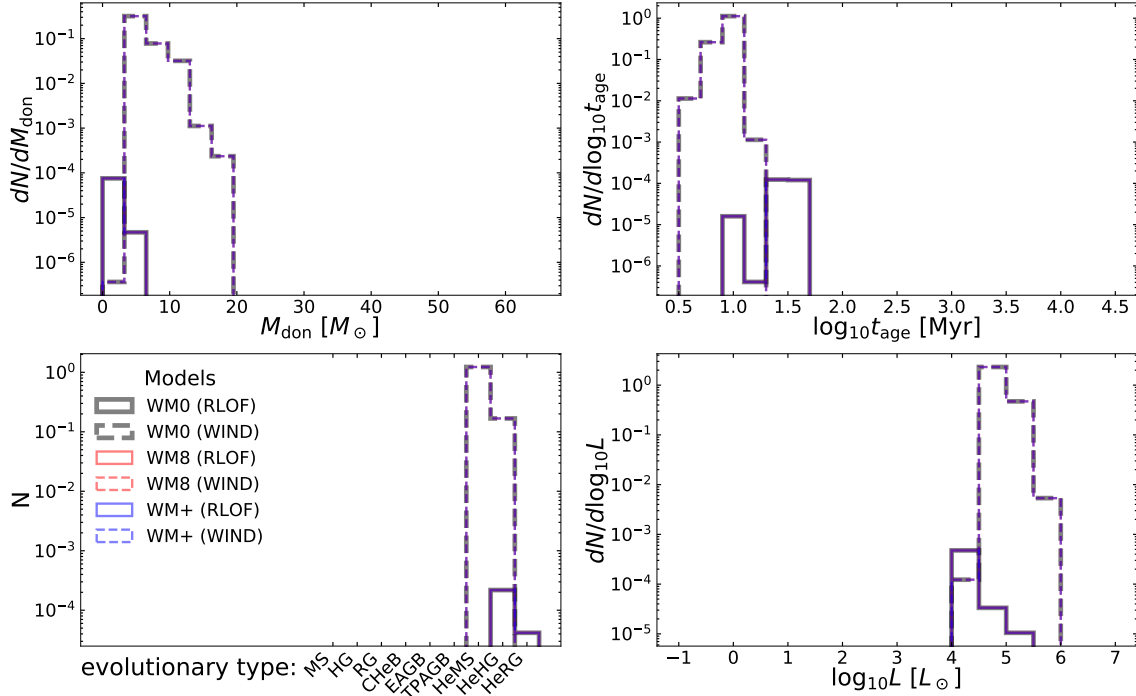


FIG. 8.— Parameter distributions of merging DCO progenitors among ULXs. Similar to Figure 7 (x-axes kept the same for easier comparison). There are no progenitors that are fed through WRLOF accretion mode, therefore, distributions for all tested models are similar.





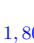









Merging DCO Progenitor Evolution					
age [Myr]		phase	$M_a [M_\odot]$	$M_b [M_\odot]$	
0	MS   MS $a \approx 380 R_\odot$; $e \approx 0.03$	ZAMS	49.0	21.6	
4.4	HG   MS $a \approx 420 R_\odot$; $e \approx 0.00$	MT	39.6 (14.3)	21.4 (25.4)	
5.0	BH   MS $a \approx 1,800 R_\odot$; $e \approx 0.00$	SN	8.14	25.2	
8.1	BH   CHeB $a \approx 4.1 R_\odot$; $e \approx 0.00$	CE	8.12	24.2	
8.4	BH   HeMS $a \approx 4.2 R_\odot$; $e \approx 0.00$	BHL	8.37 (8.56)	6.71 (5.36)	
9.1	BH   HeHG $a \approx 4.6 R_\odot$; $e \approx 0.00$	RLOF	8.56	5.36 (3.92)	
9.1	BH   NS $a \approx 9.1 R_\odot$; $e \approx 0.24$ $t_{\text{merge}} \approx 25.2 \text{ Myr}$	SN	8.56	1.45	

FIG. 9.— Same as Figure 4, but for a typical wind-fed ULX that is a progenitor of a merging DCO. Additional abbreviations (not explained in captions to Figures 4, 5, and 6), are for binary evolution: CE—common envelope binary; and for stellar evolution: HeMS—Helium main sequence; HeHG—Helium Hertzsprung gap.

donors can help us to understand the nature of ULXs, but are difficult-to-observe objects. Except for potential ULXs such as SS433 and GRS1915, all (non Be-X) ones are extragalactic objects, therefore, only the most luminous donors are bright enough to be identified by contemporary telescopes. The situations may be even worse as binary evolution studies predict that most of the companions in ULXs, especially those containing NS accretors, have low masses and are still on their MS ($\lesssim 3 M_\odot$; Wiktorowicz et al. 2017). Additionally, in most situations, the spatial coincidence of a star and an X-ray source is the only argument for physical connection. Many ULXs (especially with visible, i.e. massive, donor candidates) are localized in dense, star-forming regions, where more than one star can exist in the X-ray position error circle. What is more, the accretion disk light may exceed the optical luminosity of the donor or be hard to remove from the photometry (e.g. Grisé et al. 2012; Sutton et al. 2014). Therefore it is usually possible to look for optical counterparts only during the quiescent phases when the X-ray and optical emission from the disk is lowered.

Many authors reported the detection of stars spatially coinciding with the X-ray sources naming them as companion candidates. Motch et al. (2011) identified a potential optical counterpart to NGC7793 P13 with spectral features suggesting a supergiant luminosity class. Motch et al. (2014) estimated a mass of $18\text{--}23 M_\odot$ for this object assuming that minimum light represents the stellar light. Their modeling of the disk optical emission caused by X-ray heating supported this assumption. The

star was classified as B9Ia, which together with the orbital period of ~ 64 days suggested the presence of a compact object with a mass less than $15 M_{\odot}$. Indeed, Fürst et al. (2016) discovered that it is a magnetized NS. Heida et al. (2014) concentrated on NIR companions to nearby (< 10 Mpc) ULXs and detected 11 potential NIR companions for 62 ULXs. They claim to detect all luminous NIR sources (RSG candidates) in this volume, what gives a conclusion that only a small fraction of ULXs are possibly accompanied by RSGs. Using this sample, Heida et al. (2015) identified a potential counterpart to the ULX in NGC 253 as a RSG candidate. The authors suggest that the unusually high proper motion ($\sim 66 \text{ km s}^{-1}$ larger than average for the Galaxy) strengthens their claim that the star and the ULXs are associated, because such runaway RSGs are hard to explain otherwise. Heida et al. (2016) investigated 5 more ULXs from the Heida et al. (2014) sample and found that 2 of them are spatially coinciding with NIR sources that are compatible with being RSGs. Heida et al. (2019) identified a RSG spatially coinciding with NGC 300 ULX-1, which harbours a NS accretor (Carpano et al. 2018). For such a high mass-ratio, the orbital modulations of the donor candidate are expected to be immeasurable despite the source being the nearest ULX with a known accretor type ($D = 2.0$ Mpc; Dalcanton et al. 2009).

Liu et al. (2013) detected a WR star in the ULXs in NGC 101, which is providing MT onto the accretor through wind. The detection was based on spectroscopic analysis, so provides a stronger argument than just spatial coincidence.

For older environments the number of wind-fed ULXs is expected to drop significantly due to the short life span of supergiant stars, which constrain the majority of donors. Consequently, ULXs in old stellar populations (both RLOF- and wind-fed) are predicted to be dominated by NS accretors with low-mass donors ($\lesssim 3 M_{\odot}$; Wiktorowicz et al. 2017).

El Mellah et al. (2019) studied the importance of WRLOF on ULXs. They concentrated on two specific cases with mass ratio $q = 15$ and 2. They analysed NGC 7793 P13 and M101 ULX-1 showing that for the known orbital parameters their calculations agree with the systems being wind-fed ULXs.

4.2. Wind Accretion Efficiency

In our results, the typical accretion efficiency in wind-fed ULXs in the BHL mode is 1–2%, so only supergiants producing strong stellar wind can provide a MT rate large enough to power such a source. On the other hand, in the WRLOF mode the accretion efficiency is much larger and typically reaches 30–50%. However, for WRLOF to operate, the wind must be slow inside the RL, so again supergiants are the most promising donors. We note that 50% is a limit imposed on accretion efficiency in our reference model to avoid extrapolating the results of Mohamed (2010, see also Abate et al. 2013).

There are processes, not investigated in this study, that can decrease the efficiency of wind accretion. BHL is a simple model assuming the homogeneity of the accreted mass and a linear respective motion of the accretor and the gas. However, accretion in a binary system involves non-homogeneous winds, non-linear respective motions of the accretor and the wind-source (donor), as well as

the presence of centrifugal forces. Theuns et al. (1996) performed a smooth particle hydrodynamic simulations of wind accretion in a situation where the orbital velocity is comparable to the wind velocity and, therefore, cannot be neglected. They obtained mass accretion rates 10 times smaller than expected from the BHL prescription. Already Boffin & Zacs (1994) noted that an order of magnitude lower mass-accretion rates give better agreement with observation of enrichment in barium stars. However, in the majority of our results, the orbits of wind-fed ULXs are wide, therefore, the wind velocity is much higher than the orbital velocity and the above effects may not be so strong.

For high mass accretion rates ($\dot{M} \gtrsim \dot{M}_{\text{Edd}}$) the wake can become optically thick, which leads to instabilities effectively reducing the accretion rate due to radiation momentum and energy deposition in the flow (Taam et al. 1991). What is more, Bermúdez-Bustamante et al. (2020) showed that in AGB stars most of the wind is lost through the L2 point and forms an excretion disk around the binary, effectively reducing the MT rate.

On the other hand, detailed treatment of the accretion process may lead also to the increase of the wind accretion rates. For example, an effect that was ignored in the analytical solutions, but proved to be potentially important in hydrodynamical simulations, is the formation of an accretion disk, which can occur also in the BHL accretion mode (Theuns et al. 1996). The disk can help to reduce the angular momentum of the accretion flow and, consequently, increase the accretion rate. What is more, the accretion flow can be heated to high temperature when the gravitational energy is being released, which can result in production of highly-energetic radiation that can irradiate the donor thus increase its mass-loss rate. Unfortunately, hydrodynamical simulations cover only a small fraction of the parameter space and these results cannot be applied to a general case.

Similarly, the available hydrodynamical simulations of WRLOF accretion flows are scarce and the analytical fits like those of Abate et al. (2013) depend on restricting assumptions. Especially, the upper limit for the fraction of accreted mass can be higher than 50% and a WRLOF may smoothly convert into a RLOF when the star fills its RL.

4.3. Spatial Coincidence Probability for ULXs and RSGs

Heida et al. (2015) investigated a ULX in NGC 273 (designated as J0047) that has a spatially coinciding RSG donor candidate. They calculated the probability that J0047 and the RSG are only located in the same place on the sky by chance as $< 2.6\%$ through dividing the X-ray detection error circle (95% credibility) by the size of the observational field and multiplying this value by the number of RSGs (not-fainter than the RSG coinciding with J0047) in this field. This approach was later used for two other ULXs with spatially coinciding RSGs in Heida et al. (2016). We note that such an approach does not give a probability for spatial coincidence, which is a general concept for a population, but only an expected number of RSGs with this specific luminosity inside randomly located X-ray detection error circle for this particular field. It can be shown by performing the same

analysis for a (possibly imaginary) field with $\gtrsim 100$ times more RSGs, in which case the procedure predicts a superposition chance above 100%.

The main problem of this method is that the object chosen for investigation (J0047) was not chosen at random, but due to the coinciding RSG. This is a relatively rare situation since only several such cases were found among hundreds of known ULXs. Only the analysis of the entire populations of ULXs and RSGs, or their representative samples, may allow performing reliable statistical estimates of the probability of having a ULX and a RSG in the same position on the sky. The situation may be further complicated, however, by the fact that current observational surveys are biased towards bright NIR sources effectively favouring RSGs neglecting other unobserved stars that may be much better donor candidates.

Despite the problems pointed out above with connecting ULXs to RSGs by spatial coincidence alone, we note that our theoretical analysis presented in this paper shows that a significant fraction of the ULXs ($\sim 42\text{--}54\%$; Table 2) does possess RSG donors. Some of these sources may be hidden from our view due to misalignment of the emission beam and the line of sight.

5. SUMMARY

In this study we analysed the population of wind-fed ULXs in the context of the entire ULX population. Using population synthesis method and statistical analysis we showed that wind-fed ULXs, which were mostly neglected in previous studies, constitute a significant fraction of all ULXs and in some environments may be a majority. Although our assumptions were rather optimistic, we prove that wind-fed ULXs cannot be neglected in research on ULXs, lest the study is systematically biased. Our sample contains a significant fraction of RSG companions, thus supports the suggestion that the apparent

superposition of some ULXs and RSGs results from co-existence as a binary. Although some of these systems will evolve into DCOs, none of the ULX systems harboring a RSG donor are viable progenitors of DCO mergers with $t_{\text{merge}} < 10$ Gyr, due to the large separations.

One should stress, however, that the models of wind accretion used in our study might not be always realistic, which could influence our results. This problem can be solved only by extensive numerical simulations of wind accretion onto compact bodies in close and wide binary systems.

We are thankful to thousands of volunteers, who took part in the *Universe@Home* project⁵ and provided their computers for simulation used in this study. GW is partly supported by the President's International Fellowship Initiative (PIFI) of the Chinese Academy of Sciences under grant no.2018PM0017 and by the Strategic Priority Research Program of the Chinese Academy of Science Multi-waveband Gravitational Wave Universe (Grant No. XDB23040000). This work is partly supported by the National Natural Science Foundation of China (Grant No. 11690024, 11873056, and 11991052) and the National Key Program for Science and Technology Research and Development (Grant No. 2016YFA0400704). KB and GW acknowledge the NCN grant MAESTRO 2018/30/A/ST9/00050. This work is partly supported by the National Key Program for Science and Technology Research and Development (Grant No. 2016YFA0400704), and the National Natural Science Foundation of China (Grant No. 11690024 and 11873056). JPL was supported in part by a grant from the French Space Agency CNES. KB acknowledges support from the Polish National Science Center (NCN) grant Maestro (2018/30/A/ST9/00050).

REFERENCES

- Abate, C., Pols, O. R., Izzard, R. G., Mohamed, S. S., & de Mink, S. E. 2013, *A&A*, 552, A26
- Abbott, B. P., Abbott, R., Abbott, T. D., et al. 2016, *ApJ*, 818, L22
- Abbott, R., et al., LIGO Scientific Collaboration, & Virgo Collaboration. 2020, *ApJ*, 896, L44
- Abramowicz, M. A. 2005, in *Growing Black Holes: Accretion in a Cosmological Context*, ed. A. Merloni, S. Nayakshin, & R. A. Sunyaev, 257–273
- Bachetti, M., Harrison, F. A., Walton, D. J., et al. 2014, *Nature*, 514, 202
- Belczynski, K. 2020, *ApJ*, 905, L15
- Belczynski, K., Bulik, T., Fryer, C. L., et al. 2010a, *ApJ*, 714, 1217
- Belczynski, K., Dominik, M., Bulik, T., et al. 2010b, *ApJ*, 715, L138
- Belczynski, K., Kalogera, V., Rasio, F. A., et al. 2008, *ApJS*, 174, 223
- Belczynski, K., Klencki, J., Fields, C. E., et al. 2020, *A&A*, 636, A104
- Bermúdez-Bustamante, L. C., García-Segura, G., Steffen, W., & Sabin, L. 2020, *MNRAS*, 493, 2606
- Boffin, H. M. J., & Jorissen, A. 1988, *A&A*, 205, 155
- Boffin, H. M. J., & Zacs, L. 1994, *A&A*, 291, 811
- Bondi, H. 1952, *MNRAS*, 112, 195
- Brightman, M., Harrison, F. A., Fürst, F., et al. 2018, *Nature Astronomy*, 2, 312
- Brightman, M., Earnshaw, H., Fürst, F., et al. 2020, *ApJ*, 895, 127
- Carpano, S., Haberl, F., Maitra, C., & Vasilopoulos, G. 2018, *MNRAS*, 476, L45
- Colbert, E. J. M., & Mushotzky, R. F. 1999, *ApJ*, 519, 89
- Copperwheat, C., Cropper, M., Soria, R., & Wu, K. 2005, *MNRAS*, 362, 79
- . 2007, *MNRAS*, 376, 1407
- Dalcanton, J. J., Williams, B. F., Seth, A. C., et al. 2009, *ApJS*, 183, 67
- Dall’Osso, S., Perna, R., & Stella, L. 2015, *MNRAS*, 449, 2144
- Earnshaw, H. P., Heida, M., Brightman, M., et al. 2020, *ApJ*, 891, 153
- Edgar, R. 2004, *NAR*, 48, 843
- Ekşi, K. Y., Andaç, İ. C., Çikintoğlu, S., et al. 2015, *MNRAS*, 448, L40
- El Mellah, I., Sundqvist, J. O., & Keppens, R. 2019, *A&A*, 622, L3
- Fürst, F., Walton, D. J., Stern, D., et al. 2017, *ApJ*, 834, 77
- Fürst, F., Walton, D. J., Harrison, F. A., et al. 2016, *ApJ*, 831, L14
- Greene, J. E., Strader, J., & Ho, L. C. 2019, *arXiv e-prints*, arXiv:1911.09678
- Grisé, F., Kaaret, P., Corbel, S., et al. 2012, *ApJ*, 745, 123
- Hamann, W. R., & Koesterke, L. 1998, *A&A*, 335, 1003
- Hameury, J. M., & Lasota, J. P. 2020, *A&A*, 643, A171
- Heida, M., Jonker, P. G., Torres, M. A. P., et al. 2016, *MNRAS*, 459, 771
- . 2014, *MNRAS*, 442, 1054

⁵ <https://universeathome.pl/>

- Heida, M., Torres, M. A. P., Jonker, P. G., et al. 2015, *MNRAS*, 453, 3510
- Heida, M., Lau, R. M., Davies, B., et al. 2019, *ApJ*, 883, L34
- Höfner, S. 2007, *Astronomical Society of the Pacific Conference Series*, Vol. 378, *Headwind: Modelling Mass Loss of AGB Stars, Against All Odds*, ed. F. Kerschbaum, C. Charbonnel, & R. F. Wing, 145
- Höfner, S., & Olofsson, H. 2018, *A&A Rev.*, 26, 1
- Hoyle, F., & Lyttleton, R. A. 1939, *Proceedings of the Cambridge Philosophical Society*, 35, 405
- Hurley, J. R., Pols, O. R., & Tout, C. A. 2000, *MNRAS*, 315, 543
- Ilkiewicz, K., Mikołajewska, J., Belczyński, K., Wiktorowicz, G., & Karczmarek, P. 2019, *MNRAS*, 485, 5468
- Israel, G. L., Belfiore, A., Stella, L., et al. 2017, *Science*, 355, 817
- Ivanova, N., Justham, S., Chen, X., et al. 2013, *A&A Rev.*, 21, 59
- Kaaret, P., Feng, H., & Roberts, T. P. 2017, *ARA&A*, 55, 303
- King, A., & Lasota, J.-P. 2019, *MNRAS*, 485, 3588
- . 2020, *MNRAS*, 494, 3611
- King, A. R. 2009, *MNRAS*, 393, L41
- King, A. R., Davies, M. B., Ward, M. J., Fabbiano, G., & Elvis, M. 2001, *ApJ*, 552, L109
- Kippenhahn, R., Kohl, K., & Weigert, A. 1967, *ZAp*, 66, 58
- Kippenhahn, R., & Weigert, A. 1967, *ZAp*, 65, 251
- Lasota, J.-P., Vieira, R. S. S., Sadowski, A., Narayan, R., & Abramowicz, M. A. 2016, *A&A*, 587, A13
- Liao, Z., Liu, J., Zheng, X., & Gou, L. 2020, *MNRAS*, 492, 5922
- Licquia, T. C., & Newman, J. A. 2015, *ApJ*, 806, 96
- Liu, J.-F., Bregman, J. N., Bai, Y., Justham, S., & Crowther, P. 2013, *Nature*, 503, 500
- López, K. M., Heida, M., Jonker, P. G., et al. 2017, *MNRAS*, 469, 671
- . 2020, *arXiv e-prints*, arXiv:2006.02795
- Maxted, N. I., Ruiter, A. J., Belczynski, K., Seitzzahl, I. R., & Crocker, R. M. 2020, *arXiv e-prints*, arXiv:2010.15341
- Middleton, M. J., Brightman, M., Pintore, F., et al. 2019, *MNRAS*, 486, 2
- Middleton, M. J., Heil, L., Pintore, F., Walton, D. J., & Roberts, T. P. 2015, *MNRAS*, 447, 3243
- Mohamed, S. 2010, PhD thesis, University of Oxford, Oxford, UK
- Mohamed, S., & Podsiadlowski, P. 2007, in *Astronomical Society of the Pacific Conference Series*, Vol. 372, 15th European Workshop on White Dwarfs, ed. R. Napiwotzki & M. R. Burleigh, 397
- Mondal, S., Belczyński, K., Wiktorowicz, G., Lasota, J.-P., & King, A. R. 2020, *MNRAS*, 491, 2747
- Motch, C., Pakull, M. W., Grisé, F., & Soria, R. 2011, *Astronomische Nachrichten*, 332, 367
- Motch, C., Pakull, M. W., Soria, R., Grisé, F., & Pietrzyński, G. 2014, *Nature*, 514, 198
- Mushtukov, A. A., Suleimanov, V. F., Tsygankov, S. S., & Poutanen, J. 2015, *MNRAS*, 454, 2539
- Paczynski, B. 1971, *ARA&A*, 9, 183
- Pakull, M. W., Grisé, F., & Motch, C. 2006, in *IAU Symposium*, Vol. 230, *Populations of High Energy Sources in Galaxies*, ed. E. J. A. Meurs & G. Fabbiano, 293–297
- Pavlovskii, K., Ivanova, N., Belczynski, K., & Van, K. X. 2017, *MNRAS*, 465, 2092
- Poutanen, J., Lipunova, G., Fabrika, S., Butkevich, A. G., & Abolmasov, P. 2007, *MNRAS*, 377, 1187
- Rodríguez Castillo, G. A., Israel, G. L., Belfiore, A., et al. 2020, *ApJ*, 895, 60
- Sathyaprakash, R., Roberts, T. P., Walton, D. J., et al. 2019, *MNRAS*, 488, L35
- Shakura, N. I., & Sunyaev, R. A. 1973, *A&A*, 24, 337
- Shima, E., Matsuda, T., Takeda, H., & Sawada, K. 1985, *MNRAS*, 217, 367
- Sutton, A. D., Done, C., & Roberts, T. P. 2014, *MNRAS*, 444, 2415
- Swartz, D. A., Soria, R., Tennant, A. F., & Yukita, M. 2011, *ApJ*, 741, 49
- Taam, R. E., Fu, A., & Fryxell, B. A. 1991, *ApJ*, 371, 696
- Tetarenko, B. E., Sivakoff, G. R., Heinke, C. O., & Gladstone, J. C. 2016, *The Astrophysical Journal Supplement Series*, 222, 15
- Theuns, T., Boffin, H. M. J., & Jorissen, A. 1996, *MNRAS*, 280, 1264
- Tong, H. 2015, *Research in Astronomy and Astrophysics*, 15, 517
- van den Heuvel, E. P. J., Portegies Zwart, S. F., & de Mink, S. E. 2017, *MNRAS*, 471, 4256
- Vink, J. S. 2008, *NAR*, 52, 419
- Vink, J. S., & de Koter, A. 2002, *A&A*, 393, 543
- . 2005, *A&A*, 442, 587
- Vink, J. S., de Koter, A., & Lamers, H. J. G. L. M. 2001, *A&A*, 369, 574
- Walton, D. J., Roberts, T. P., Mateos, S., & Heard, V. 2011, *MNRAS*, 416, 1844
- Walton, D. J., Bachetti, M., Fürst, F., et al. 2018, *ApJ*, 857, L3
- Wiktorowicz, G., Lasota, J.-P., Middleton, M., & Belczynski, K. 2019a, *ApJ*, 875, 53
- Wiktorowicz, G., Sobolewska, M., Lasota, J.-P., & Belczynski, K. 2017, *ApJ*, 846, 17
- Wiktorowicz, G., Sobolewska, M., Sądowski, A., & Belczynski, K. 2015, *ApJ*, 810, 20
- Wiktorowicz, G., Wyrzykowski, Ł., Chruslinska, M., et al. 2019b, *ApJ*, 885, 1
- Zdziarski, A. A. 2014, *MNRAS*, 444, 1113